Magnetostructural Correlations in Parallel Square-planar Chloride Bridged Copper(II) Dimers: Structure, Dynamic Nuclear Magnetic Resonance Study, and Magnetic Properties of $[Cu_2(terpy)_2Cl_2][PF_6]_2$†

Teofilo Rojo,* Maria I. Arriortua, and Javier Ruiz
Departamentos de Quimica y Cristalografia, Facultad de Ciencias, Universidad del Pais Vasco, Bilbao, Spain
Jacques Darriet and Gerard Villeneuve
Laboratoire de Chimie du Solide du C.N.R.S., 351 Cours de la Liberation, 33405 Talence Cedex, France
Daniel Beltran-Porter
Departamento de Quimica Inorganica, Facultad de Ciencias Quimicas, Universidad de Valencia, Valencia, Spain

The crystal and molecular structure of $[Cu_2(terpy)_2Cl_2][PF_6]_2$ (terpy = 2,2′:6′,2″-terpyridyl) has been determined from three-dimensional *X*-ray data. The complex crystallizes in the monoclinic space group $P2_1/a$ with two dimeric formula units in a unit cell of dimensions a = 20.420(8), b = 13.383(1), c = 6.316 5(7) Å, and β = 97.42(4)°. The structure was determined by Patterson and Fourier methods and refined by full-matrix least-squares methods to R' = 0.054 from 715 independent reflections with $I \geqslant 2\sigma(I)$. The copper ion in each $[Cu(terpy)Cl]^+$ monomer is slightly shifted ($\simeq$0.1 Å) from the plane defined by the chlorine and the three nitrogen atoms of the terpy ligand. Interactions between monomer units *via* long copper–chlorine bonds create discrete dibridged cationic species. Reorientations of the PF_6^- groups in the solid are discussed on the basis of ^{19}F and ^{31}P n.m.r. spectroscopic results. High-field magnetization measurements down to 2 K show the salt to be antiferromagnetically coupled and allow an evaluation of the singlet–triplet energy gap ($2J = -5.9$ cm^{-1}). The magnetic behaviour of this complex and other di-μ-chloro bridged parallel planar dimers is discussed on the basis of correlations with structural data.

There has been considerable interest in correlating the structural characteristics and magnetic properties of dimeric bridged copper(II) complexes. A large amount of theoretical and experimental work has been carried out in the investigation of systems where the bridging atoms are oxygen, but in recent years several research groups have undertaken systematic studies of the magnetostructural correlations of di-μ-halogeno bridged copper(II) dimers.

The chloride bridged copper(II) dimers are capable of assuming a number of different co-ordination geometries which involve various orbitals in the superexchange.[1] Thus it is not surprising that the theoretical calculations for these dimers predict different magnetic behaviours for each symmetry type. One cannot expect to find a general magnetostructural correlation similar to the simple one detected for the di-μ-hydroxo bridged copper dimers,[2] and each type of dimer must be discussed separately.

In this paper the crystal structure and magnetic properties of a new parallel square-planar copper(II) dimer are discussed. The role played by structural parameters other than the bridging angle is discussed in relation to the magnetic properties of the complex and other known dimers having the same geometry.

Experimental

2,2′:6′,2″-Terpyridyl (terpy, $C_{15}H_{11}N_3$) was purchased from G. F. Smith Chem. Co. Inc.; Merck $CuCl_2 \cdot 2H_2O$ and KPF_6 were used without further purification.

Preparation.—Samples of $[Cu_2(terpy)_2Cl_2][PF_6]_2$ were prepared by addition of an excess of a KPF_6 saturated aqueous solution to a warm aqueous solution (0.8 g in 20 cm^3) of $[Cu(terpy)Cl_2] \cdot H_2O$. Synthesis of the latter complex has been previously described.[3] A blue precipitate was separated by vacuum filtration and readily recrystallized from a saturated aqueous solution. The crystals were isolated after filtration, washed with distilled water, and dried over P_2O_5 for 24 h. The resulting crystals were blue needles and of relatively good quality (Found: C, 37.90; H, 2.35; Cu, 13.55; N, 8.70. Calc. for $C_{15}H_{11}ClCuF_6N_3P$: C, 37.75; H, 2.30; Cu, 13.30; N, 8.80%).

Physical Measurements.—Transmission and reflectance spectra were obtained from a Pye-Unicam SP8-100 spectrometer. Infrared spectra were recorded with a Pye-Unicam SP2000 from KBr discs.

Variable-temperature (4.2—300 K) magnetic susceptibility and e.s.r. measurements were performed as described in a recent paper.[4a]

Magnetization measurements up to 15 T and at temperatures down to 2 K were performed at the C.N.R.S. Service National des Champs Intenses (Grenoble).

The ^{19}F and ^{31}P n.m.r. studies were carried out by continuous wave (c.w.) methods at 16 MHz, using a cross-coil Bruker SWL 3-100 spectrometer. The Zeeman magnetic field was supplied by a Drusch magnet monitored by a Hall probe. The sweep was calibrated by a Bruker BNM 20 gaussmeter. Care was taken to avoid saturation, using various small r.f. powers. The temperature was controlled with a conventional gas-flow system blowing the sample.

The experimental second moments have been determined by numerical integration for the recordings of the first derivative of the absorption line, corrected for finite modulation amplitude, H_m.

† Di-μ-chloro-bis[(2,2′:6′,2″-terpyridyl)copper(II)] bis(hexafluorophosphate).

Supplementary data available: see Instructions for Authors, *J. Chem. Soc., Dalton Trans.*, 1987, Issue 1, pp. xvii—xx.

Non-S.I. unit employed: G = 10^{-4} T.

Table 1. Final positional parameters for the non-hydrogen atoms in $[Cu_2(terpy)_2Cl_2][PF_6]_2$ *

Atom	x	y	z	B_{eq}/Å^2
Cu	0.073 9(11)	0.068 5(2)	0.030 4(4)	2.70(10)
Cl	0.041 0(2)	−0.050 7(4)	−0.203 2(8)	3.19(12)
P	0.327 4(4)	0.099 9(4)	0.108 1(11)	3.28(12)
F(1)	0.358 4(9)	0.204 7(12)	0.127 3(26)	8.46(33)
F(2)	0.396 4(8)	0.057 6(14)	0.191 8(37)	16.19(76)
F(3)	0.259 2(10)	0.143 2(15)	0.025 7(31)	11.20(38)
F(4)	0.338 2(8)	0.094 5(13)	−0.129 5(24)	5.87(14)
F(5)	0.312 7(9)	0.112 7(14)	0.339 4(26)	6.39(14)
F(6)	0.296 4(10)	−0.006 8(11)	0.091 7(28)	9.08(35)
N(1)	0.107 2(9)	0.171 6(15)	0.223 8(31)	3.34(15)
N(2)	0.039 6(8)	0.188 4(12)	−0.146 6(30)	3.00(13)
N(3)	0.131 8(8)	−0.012 6(17)	0.249 4(27)	3.44(16)
C(1)	0.095 7(9)	0.269 7(21)	0.166 9(33)	2.99(12)
C(2)	0.114 4(12)	0.348 9(17)	0.306 1(42)	3.67(14)
C(3)	0.152 3(13)	0.321 7(21)	0.499 6(45)	4.73(22)
C(4)	0.168 8(10)	0.225 0(25)	0.557 0(33)	3.79(14)
C(5)	0.145 6(10)	0.146 6(20)	0.405 4(40)	3.54(16)
C(6)	0.159 0(11)	0.040 0(23)	0.427 5(45)	3.42(13)
C(7)	0.193 0(11)	−0.005 7(23)	0.603 4(39)	3.34(12)
C(8)	0.203 7(11)	−0.107 9(24)	0.597 0(44)	5.75(27)
C(9)	0.174 7(12)	−0.167 7(21)	0.420 6(46)	4.91(20)
C(10)	0.138 7(11)	−0.110 5(23)	0.247 6(40)	4.75(23)
C(11)	0.052 6(10)	0.275 9(20)	−0.037 0(38)	3.68(16)
C(12)	0.027 2(10)	0.367 2(17)	−0.129 3(40)	4.99(25)
C(13)	−0.011 7(11)	0.362 3(25)	−0.337 1(42)	4.82(18)
C(14)	−0.023 8(11)	0.270 1(22)	−0.442 2(43)	5.45(26)
C(15)	0.004 3(11)	0.185 4(18)	−0.343 5(37)	2.55(08)

* $B_{eq} = \frac{8}{3}\pi^2(U_{11} + U_{22} + U_{33} + 2U_{13}\cos\beta)$.

Crystal Structure Determination of $[Cu_2(terpy)_2Cl_2][PF_6]_2$.—*Crystal data.* $C_{15}H_{11}ClCuF_6N_3P$, $M = 477.3$, monoclinic, $a = 20.420(8)$, $b = 13.383(1)$, $c = 6.316\,5(7)$ Å, $\beta = 97.42(4)°$, $U = 1\,712$ Å^3 (by least-squares refinement on diffractometer angles for 25 automatically centred reflections, $\lambda = 0.710\,69$ Å), space group $P2_1/a$, $Z = 4$, $D_c = 1.851$ kg m^{-3}. Crystal dimensions: 0.04 × 0.05 × 0.77 mm, λ(Mo-K_α) = 16.36 cm^{-1}, $F(000) = 948$.

Data collection and processing. The intensities of 2 086 independent reflections ($2\theta \leqslant 50°$) were measured using a Philips PW 1100 four-circle diffractometer with graphite-monochromatized Mo-K_α radiation. 715 Reflections corresponding to $I \geqslant 2\sigma(I)$ were considered observed and used in the refinement. Lorentz and polarization corrections were applied.

Structure analysis and refinement. The copper and chlorine positions were determined from a three-dimensional Patterson map. The positions of the non-hydrogen atoms were from a series of Fourier syntheses based on the Cu and Cl positions. Structure refinement proceeded using full-matrix least-squares treatment of the overall scale factors and the individual positional and anisotropic thermal parameters for all 27 non-hydrogen atoms.

Several cycles of refinement led to convergence with $R = 0.056$ and $R' = 0.054$ $\{R = \Sigma(|F_o| - |F_c|)/\Sigma|F_o|$ and $R' = [\Sigma w(|F_o| - |F_c|)^2/\Sigma wF_o]^{\frac{1}{2}}\}$. Final atomic positional parameters are listed in Table 1.

The *X*-RAY 70 system of computer programs[4b] was used for the structure determination.

Results and Discussion

Figure 1 shows a view of the dimeric cation $[Cu_2(terpy)_2Cl_2]^{2+}$. Bond distances and angles are given in Table 2.

Each copper ion in the dimer is clearly five-co-ordinated with approximate square-pyramidal geometry. Four of the co-ordinating atoms, *i.e.* a chlorine atom and the three nitrogen atoms of a terpy ligand, do in fact lie at the corners of a distorted square plane around the copper ion. The second chlorine atom (Cl′) occupies the apical position of the pyramid.

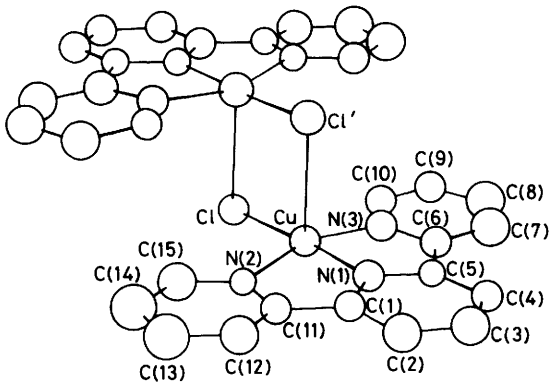

Figure 1. View of the $[Cu_2(terpy)_2Cl_2]^{2+}$ dimeric unit

The two outer nitrogen atoms [N(2) and N(3)] lie further from the copper ion (2.02 Å) than the central nitrogen atom [N(1)] (1.91 Å). This implies a deformation of the interatomic angles between atoms of adjacent pyridine rings, and leads to a small departure from planarity of the ligands. The same pattern of bond distances and angle deformation has been observed in most terpy complexes with copper(II)[5-10] or other divalent transition-metal ions.[11-13]

The copper–chlorine apical bond is much longer than the basal one [2.723(38) *vs.* 2.218(19) Å], a feature which appears frequently in copper crystal chemistry, and which characterizes the square-pyramidal configuration. The same feature has been observed in the monomer $[Cu(terpy)Cl_2]\cdot H_2O$,[3] but the Cu–Cl bond length difference is bigger in the present dimer than in the monomeric complex (0.505 *vs.* 0.334 Å) reflecting the slight out-of-basal plane displacement of the copper ion in $[Cu_2(terpy)_2Cl_2]^{2+}$ with respect to the monomer (0.1 *vs.* 0.4 Å).

The PF_6^- anion appears to be a regular octahedron with normal bond distances and angles, as expected from i.r. data (no splitting is observed for ν_3 and ν_4 i.r. absorption bands which appear at 840 and 560 cm^{-1} respectively). However, the isotropic thermal parameters of the fluorine atoms are too high when compared with those found for the other atoms (Table 1). The same behaviour has been observed for the PF_6^- ion in other terpy co-ordination compounds.[6,14] This result accounts for the existence of mobility of the fluorine atoms.

To study the atom motion on the basis of crystallographic data (by rigid motion decomposition analysis, for example) very accurate corrected values of the anisotropy parameters are required.[15,16] Therefore, this problem has been confronted using n.m.r. spectroscopy instead.

N.M.R. Study of Fluorine Motion in the PF_6^- *Anion.*—N.m.r. will provide valuable information about the dynamic state of the PF_6^- ion from the analysis of the second moment of the absorption line. The shape of the ^{19}F absorption line is shown in Figure 2(*a*). Neither width nor shape variation is observed between 200 and 450 K. The experimental fluorine second moment corresponding to this line is 0.96(3) G^2.

The theoretical second moment produced by magnetic dipole–dipole interactions can be calculated from Van Vleck's treatment of a rigid lattice.[17] For a polycrystalline sample it may be written as equation (1), where indices *i* and *j* refer to the

$$M_2 = \tfrac{3}{5}[\gamma_i^2\hbar^2 I_i(I_i + 1)\, N^{-1}\sum_{i,j} r_{ij}^{-6}] + \tfrac{4}{15}[\hbar^2\, N^{-1}\sum_{i,k}\gamma_k^2 I_k(I_k + 1)\, r_{ik}^{-6}] \quad (1)$$

Table 2. Molecular distances (Å) and angles (°) for $[Cu_2(terpy)_2Cl_2][PF_6]_2$

N(1)–C(1)	1.373(34)	C(12)–C(13)	1.445(44)	F(1)–F(2)	2.136(25)
N(1)–C(5)	1.345(40)	C(13)–C(14)	1.408(43)	F(1)–F(3)	2.204(35)
N(2)–C(11)	1.369(31)	C(14)–C(15)	1.382(38)	F(1)–F(4)	2.192(26)
N(2)–C(15)	1.355(39)	C(1)–C(11)	1.465(42)	F(1)–F(5)	2.122(35)
N(3)–C(6)	1.381(38)	Cu–N(1)	1.909(26)	F(1)–F(6)	3.097(23)
N(3)–C(10)	1.318(38)	Cu–N(2)	2.028(23)	F(2)–F(3)	3.083(46)
C(1)–C(2)	1.398(36)	Cu–N(3)	2.017(37)	F(2)–F(4)	2.270(50)
C(2)–C(3)	1.407(45)	Cu–Cl	2.218(19)	F(2)–F(5)	2.178(40)
C(3)–C(4)	1.374(43)	Cu–Cl′	2.723(38)	F(2)–F(6)	2.231(34)
C(4)–C(5)	1.458(39)	Cu–Cu′	3.510(14)	F(3)–F(4)	2.097(41)
C(5)–C(6)	1.456(40)	P–F(1)	1.537(18)	F(3)–F(5)	2.174(47)
C(6)–C(7)	1.375(43)	P–F(2)	1.547(27)	F(3)–F(6)	2.168(26)
C(7)–C(8)	1.386(44)	P–F(3)	1.536(28)	F(4)–F(5)	3.082(31)
C(8)–C(9)	1.436(43)	P–F(4)	1.547(19)	F(4)–F(6)	2.197(33)
C(9)–C(10)	1.454(43)	P–F(5)	1.539(22)	F(5)–F(6)	2.232(26)
C(11)–C(12)	1.423(35)	P–F(6)	1.560(17)		

N(1)–Cu–N(2)	81.4(8)	N(1)–C(1)–C(2)	122(2)	C(1)–C(2)–C(3)	115(2)
N(1)–Cu–N(3)	79.7(8)	C(2)–C(3)–C(4)	124(2)	C(3)–C(11)–C(5)	122(1)
N(2)–Cu–Cl	98.6(5)	C(4)–C(5)–N(1)	119(2)	C(5)–N(1)–C(1)	121(2)
N(3)–Cu–Cl	99.8(6)	N(2)–C(11)–C(12)	119(2)	C(11)–C(12)–C(13)	118(2)
N(1)–Cu–Cl	176.5(6)	C(12)–C(13)–C(14)	121(3)	C(13)–C(14)–C(15)	118(2)
Cl′–Cu–N(1)	94.5(6)	C(14)–C(15)–N(2)	122(2)	C(15)–N(2)–C(11)	122(2)
Cl′–Cu–N(2)	92.1(5)	N(3)–C(6)–C(7)	123(3)	C(6)–C(7)–C(8)	119(2)
Cl′–Cu–N(3)	97.9(5)	C(7)–C(8)–C(9)	121(2)	C(8)–C(9)–C(10)	114(2)
Cl′–Cu–Cl	90.1(2)	C(9)–C(10)–N(3)	124(2)	C(10)–N(3)–C(6)	119(2)

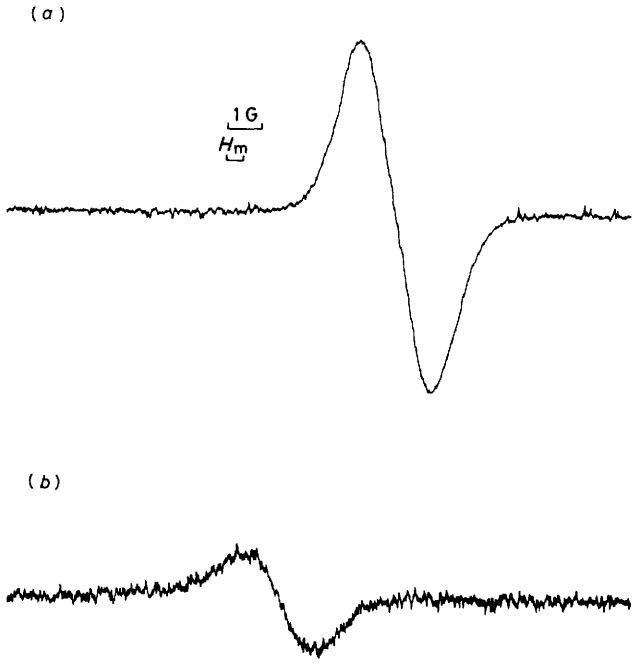

Figure 2. (*a*) First derivative of the absorption line of ^{19}F at 16 MHz. The scale and the amplitude of the modulation (H_m) are given. (*b*) First derivative of the absorption line of ^{31}P

nuclei giving rise to the absorption concerned and k to other magnetic nuclei in the material; I is the nuclear spin, γ the gyromagnetic ratio, N the number of resonant nuclei, r_{ij} and r_{ik} are the internuclear distances.

The dipole–dipole broadening of the line is due to intragroup interactions (F–F and F–P) for the PF_6^- ion and also to the interactions with all the other magnetic nuclei (F and P located in the other PF_6^- ions, Cu, N, Cl, H). We call the latter 'intergroup' or 'extra' interactions.

Using equation (1) it is possible to calculate the intragroup contribution to the second moment for a rigid lattice. As a first approximation we neglect the distortion of the octahedron and take the average value of the interatomic distances given in Table 2: 4 ⟨F–F⟩ = 2.182, 1 ⟨F–F⟩ = 3.086, and 6 ⟨F–P⟩ = 1.543 Å. This gives a calculated second moment M_2(intra) = 13.94 G^2 (12.01 G^2 for the F–F interactions, 1.93 G^2 for the F–P ones). A more precise result is obtained by taking into account the distances obtained from the crystallographic data themselves. The value thus obtained is then 14.11 G^2 (12.18 + 1.93). The relative difference, $\Delta M_2/M_2$, in percentage terms is 1.2%. Equation (1) shows in fact that the second moment is very sensitive to the interatomic distances ($\Delta M_2/M_2 = 6\,\Delta r/r$). The mean standard deviation $\Delta r/r$ is 1.2×10^{-2} and corresponds to $\Delta M_2/M_2 = 7\%$, a value six times larger than the difference introduced by the distortion. Afterwards we shall neglect the distortion of the octahedron. The total second moment is larger than M_2(intra), but this contribution alone is $\simeq 15$ times higher than the experimental value $M_2 = 0.96$ G^2. This fact clearly indicates that the PF_6^- ions are not rigid but have a dynamic behaviour. When a group reorients itself at a frequency large enough compared with the linewidth (expressed in frequency units), the second moment is reduced and the reduction factor can be calculated if the mechanism of the motion is known. In order to explain the experimental results we shall now consider the possible mechanisms which are able to occur in an octahedron.

Reorientations of the PF_6^- *groups around a symmetry axis.* The simplest motions which could narrow the fluorine resonance line are reorientations of the PF_6^- groups about the (pseudo) two-, three-, and four-fold symmetry axes. For such a mechanism the second moment would be reduced by the factor $\frac{1}{4}(3\cos^2\nu_{ij} - 1)^2$ where ν_{ij} is the angle between the internuclear vector r_{ij} and the rotation axis. Table 3 gives the relative intragroup contributions to the ^{19}F second moment of the F–F interactions in the three cases.

In each case the total contribution, even without taking into account the intergroup interactions, is much too large compared to the experimental value (0.96 G^2).

Table 3. Second moment (in G^2) of the ^{19}F line calculated for a rotation of the PF_6^- group around a single axis

Rotation axis	F–F contribution	F–P contribution	Total
C_2	2.61	0.24	2.85
C_3	2.93	0	2.93
C_4	1.65	0.96	2.61

Table 4. Contribution to the second moment (in G^2) of the ^{19}F line calculated for a spherical rotation of the PF_6^- group

Interaction	F–F	F–P	F–Cu	F–N	F–Cl	Total
M_2/G^2	0.120	0.002	0.009	0.002	0.0006	0.133

Spherical rotation. In this model the PF_6^- group is assimilated to a sphere which reorientates itself at random around a continuous range of axes. As a consequence the intragroup interactions average out to zero and we are left with the 'extra' or 'intergroup' interactions (*i.e.* PF_6–PF_6, F–Cu, F–N, F–Cl, and F–H). McCall and Douglas [18] have shown that for spherical rotation the intergroup interactions are equivalent to the rigid lattice values obtained by placing each nucleus at the centre of the sphere, in our case at the phosphorus positions. Then, from the knowledge of the atomic positions and Van Vleck's relation, it is easy to calculate all the different contributions to the second moment except the F–H one since the proton positions are unknown. Table 4 gives the results obtained.

The difference between the observed value and the calculated one [$\Delta M_2 = 0.83(3)\ G^2$] could be ascribed to the contribution of the F–H interactions. In order to confirm this hypothesis, ^{31}P nuclear resonance has been carried out [Figure 2(*b*)]. The observed second moment is $0.86(5)\ G^2$. As for the ^{19}F nuclei, the ^{31}P intragroup dipolar interactions are averaged out by a spherical rotation. The contributions from foreign nuclei (Cu, N, Cl, and H) are the same for both ^{19}F and ^{31}P second moments [see equation (1)]. The only difference comes from the interactions involving the ^{19}F and ^{31}P nuclei, equation (2).

$$\Delta M_2 = M_2(^{19}F) - M_2(^{31}P) = M_2(F\text{-}F) + M_2(F\text{-}P) - M_2(P\text{-}P) + M_2(P\text{-}F) \quad (2)$$

The F–F and F–P contributions are given in Table 4. The P–P and F–P ones obtained by a similar procedure are respectively 0.004 and 0.053 G^2, giving a theoretical value of $\Delta M_2 = 0.062\ G^2$, which is in excellent agreement with the experimental value ($\Delta M_2 = 0.1\ G^2$).

Although the spherical rotation of PF_6^- ions agrees well with the experimental results, the structural conclusions obtained from *X*-ray diffraction do not corroborate it: instead of giving a spherical distribution of fluorine atoms it locates them rather in six well defined positions, with anomalous high thermal parameters (Table 1). It follows that some particular positions of the F^- ions should be more probable than others.

Random reorientation of PF_6^- *group about the axis of symmetry.* Miller and Gutowsky [19] were the first to suggest this type of restricted rotation model. The simplest one is a six position model, in which a fluorine atom occupies six relatively localized positions in the crystal lattice. Reorientations would be restricted to rotations around the symmetry axes of the group, at random, with the net effect that each fluorine spends $\frac{1}{6}$ of the time in each position. The main point is that the PF_6^- ion jumps from one discrete orientation to another (identical one) at a speed fast enough to be able to neglect the transit time. Miller and Gutowsky have shown that this model gives nearly the same results (within 5%) as the spherical rotation model. Furthermore the ^{31}P resonance cannot solve the problem as the two types of reorientation have the same effect (within the range of experimental error) on the second moment.

In conclusion, n.m.r. itself cannot give a definitive idea as to the behaviour of the PF_6^- group but, with the help of *X*-ray diffraction techniques, this study may lead to a coherent interpretation of the reorientation of the PF_6^- octahedron.

Magnetic Behaviour.—We previously reported magnetic susceptibility and e.s.r. data at various temperatures for $[Cu_2(terpy)_2Cl_2][PF_6]_2$.[4] This compound exhibits resulting antiferromagnetic exchange interactions. The susceptibility data were least-squares fitted to the Bleaney–Bowers equation for isotropic spin exchange in Cu^{II} dimers. The estimation of the values of the anisotropic exchange parameters from a simple point-dipole model gives $D_\alpha \simeq 0.016\ cm^{-1}$ and $J_\alpha \simeq 0.001\ cm^{-1}$. Thus it was considered reasonable to neglect this effect and to consider simply an isotropic exchange parameter in the Heisenberg–Dirac–van Vleck (HDvV) Hamiltonian. From this fit the best values for the exchange and g parameters were $-2.47\ cm^{-1}$ and 2.116 respectively.

In this way it is considered that $[Cu_2(terpy)_2Cl_2][PF_6]_2$ acts magnetically as an assembly of isolated, non-interacting dimers. In a zero magnetic field the system is described by a singlet ground state ($S = 0$) and a triplet excited state ($S = 1$) $2J$ in energy above the singlet, S being the total spin of the pair. The behaviour in a magnetic field, described by the Hamiltonian $\mathcal{H} = -2JS_1S_2 - g\mu_BH(S_1 + S_2)$, is quite straightforward. The Zeeman splitting of the triplet state leads to a level crossing that occurs when the field reaches the values $H_c = (2|J|)/g\mu_B$, the state $|1,1\rangle$ becoming the ground state at fields higher than H_c.

If the level separation in the dimer is accessible to available magnetic fields, magnetization measurements must allow us to observe this level crossing.

The isothermal magnetization (σ) is given by equation (3),

$$\sigma = NkT\frac{\delta}{\delta H}\ln Z \quad (3)$$

where Z is the partition function: $Z = \sum_s \sum_{s_z} e^{-W_s/kT}$ and $W_s = E_s - g\mu_BHS_z$ (E_s is the energy of the S states in a zero field). For a copper(II) antiferromagnetic dimer the energy levels are $E_0 = 0$ and $E_1 = -2J$.

The expression of the magnetization becomes equation (4),

$$\sigma = N_g\mu_B\frac{(\sinh 2x - 2\sinh x)\,e^{2J/kT}}{2\sinh(x/2)[\sinh(x/2) + \sinh(3x/2)e^{2J/kT}]} \quad (4)$$

where $x = g\mu_BH/kT$. The magnetization calculated from this equation has a sigmoidal shape at low temperature ($T < 2|J|/k$). The level crossing field (H_c), and hence the energy level splitting, is determined by the inflection point.

Magnetization measurements at 2 K and applied magnetic fields up to 15 T are represented in Figure 3. A sharp increase of σ is observed which corresponds to the level crossing. Experimental magnetization data have been fitted from equation (4). The best fit has been obtained for $J = -2.95\ cm^{-1}$ and $g = 2.1$ (the calculated values are represented in Figure 3 by a dashed line). This result agrees satisfactorily with those obtained from e.s.r. and susceptibility data.

Magnetostructural Correlations.—2,2′:6′,2″-Terpyridyl as a chelating tridentate ligand allows the obtention of five-coordinate compounds of general formula $[M(terpy)X_2]$ (M = a

Table 5. Values of the different angles (°) considered in Figure 4 for various copper(II) dimers

Dimer[a]	R/Å	α_1	α_2	α_3	β_1	β_2	β_3	Φ/R/° Å^{-1}	$\alpha_1/2R$/° Å^{-1}	$2J$/cm^{-1}	Geometry	*trans* Ligand atom	Ref.
(1) [{Cu(H_2dmg)Cl_2}$_2$]	2.698	166.7	96.8	92.0	165.9	92.3	95.6	32.62(0.10)	30.9(0.10)	+0.61	sp[b]	N	*c*
(2) [{Cu(dmen)Cl_2}$_2$]	2.734	167.7	95.1	93.9	173.6	98.2	88.1	31.5(0.08)	30.7(0.08)	−2.10	sp	N	*d*
(3) [{Cu(terpy)Cl}$_2$][PF_6]$_2$	2.720	176.1	93.8	90.1	170.0	92.1	173.1	33.0(0.50)[d]	32.4(0.50)[d]	−5.90	sp	N	This work
(4) [{Cu(Hgua)Cl_3}$_2$]	2.447	94.0	95.0	82.0	112.0	114.0	134.0	40.01(0.20)	—	−82.6	tbp	Cl	*e*
(5) [{Cu(teen)Cl_2}$_2$]	2.728	185.1	91.02	85.2	145.7	111.0	103.0	34.75(0.03)	33.9(0.03)	+0.1	spth[f]	N	*g*
(6) [Co(en)$_3$][Cu_2Cl_8]Cl_2	2.703	187.4	87.8	84.8	145.3	118.3	96.3	35.22(0.10)	34.7(0.10)	−14.6	spth	Cl	*h*
(7) [{Cu(tmso)Cl_2}$_2$]	3.020	145.7	122.8	91.5	165.2	92.1	92.8	29.30(0.20)	24.1(0.20)	−17.0	sptr[f]	Cl	*i*
(8) [{Cu(tmen)Cl_2}$_2$]	3.147	189.2	88.4	83.2	157.5	105.9	96.4	30.76(0.20)	30.1(0.20)	−5.6	spth	N	*j*
(9) [{Cu(2Me-py)$_2Cl_2$}$_2$]	3.364	177.6	98.2	79.2	173.4	91.8	94.8	29.91(0.02)	26.4(0.02)	−7.4	sp	Cl	*k*
(10) [{Cu(mox)$_2Cl_2$}$_2$]	2.598	159.0	110.5	90.5	174.5	93.1	92.2	34.43(0.02)	30.6(0.02)	−2.6	sptr	Cl	*l*

[a] Abbreviations: H_2dmg = dimethylglyoxime, dmen = *N*,*N*-dimethylethylenediamine, terpy = 2,2′:6′,2″-terpyridyl, gua = guanine, teen = *N*,*N*,*N*′-triethylethylenediamine, en = ethylenediamine, tmso = tetramethylene sulphoxide, tmen = *N*,*N*,*N*′,*N*′-tetramethylethylenediamine, 2Me-py = 2-methylpyridine, mox = 4-methyl-1,3-oxazole; sp = regular square pyramid, tbp = trigonal bipyramid, spth = tetrahedral distorted square pyramid, and sptr = trigonal distorted square pyramid. [b] The ideal bond angles for the sp topology are: α_i = 165.0, 97.5, 97.5; β_i = 165.0, 97.5, 97.5°. [c] D. H. Svedung, *Acta Chem. Scand.*, 1969, **23**, 2865; M. Megnamisi-Belombe and M. A. Novotny, *Inorg. Chem.*, 1980, **19**, 2470. [d] D. W. Phelps, W. H. Goodman, and D. J. Hodgson, *Inorg. Chem.*, 1976, **15**, 2266. [e] J. A. Carrabine and M. Sundaralingam, *J. Am. Chem. Soc.*, 1970, **92**, 369; J. P. DeClercq, M. Debboudt, and M. Van Meersche, *Bull. Soc. Chim. Belg.*, 1971, **80**, 527; M. Sundaralingam and J. A. Carrabine, *J. Mol. Biol.*, 1971, **61**, 287; R. F. Drake, V. H. Crawford, N. W. Laney, and W. E. Hatfield, *Inorg. Chem.*, 1974, **13**, 1246; J. F. Villa, *ibid.*, 1973, **12**, 2054. [f] The ideal bond angles for the spth and sptr topologies are: spth (α_i; β_i) = (190, 85, 85; 140, 110, 110) and sptr (α_i; β_i) = (140, 110, 110; 170, 95, 95°). The observed deviations in Φ/R and $\alpha_1/2R$ do not modify the conclusions of the present work significantly. [g] W. E. Marsh, K. C. Patel, W. E. Hatfield, and D. J. Hodgson, *Inorg. Chem.*, 1983, **22**, 511. [h] D. J. Hodgson, P. K. Hale, and W. E. Hatfield, *Inorg. Chem.*, 1971, **10**, 1061; J. A. Barnes, W. E. Hatfield, and D. J. Hodgson, *Chem. Phys. Lett.*, 1970, **7**, 374; K. T. McGregor, D. B. Losee, D. J. Hodgson, and W. E. Hatfield, *Inorg. Chem.*, 1974, **13**, 756. [i] D. D. Swank, G. F. Needham, and R. D. Willett, *Inorg. Chem.*, 1979, **18**, 761. [j] E. D. Estes and W. E. Hatfield, *Inorg. Chem.*, 1975, **14**, 106. [k] W. E. Marsh, W. E. Hatfield, and D. J. Hodgson, *Inorg. Chem.*, 1982, **21**, 2679; W. F. Duckworth and N. C. Stephenson, *Acta Crystallogr., Sect. B*, 1969, **25**, 1795; D. Y. Jeter, D. J. Hodgson, and W. E. Hatfield, *Inorg. Chim. Acta*, 1971, **5**, 257. [l] W. E. Marsh, D. S. Eggleston, W. E. Hatfield, and D. J. Hodgson, *Inorg. Chim. Acta*, 1983, **70**, 137.

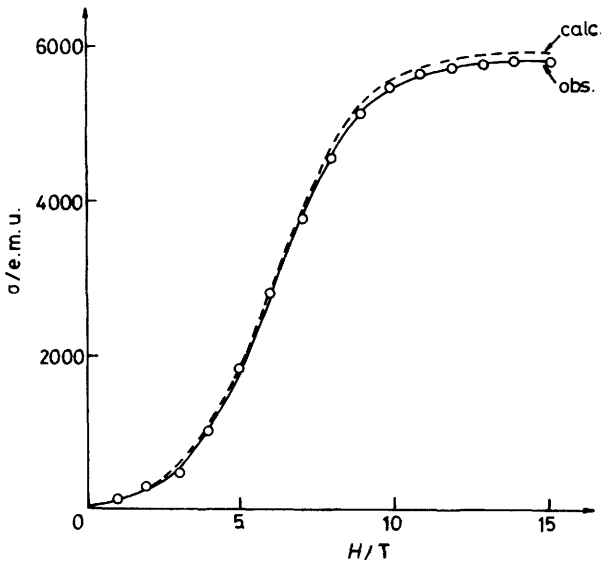

Figure 3. Variation of magnetization with applied magnetic field at T = 2 K

divalent 3*d* transition-metal ion, X = halogen or pseudohalogen anion).[3,6,10,20–23]

The environment of the central ion has at the upmost C_{2v} symmetry due to ligand rigidity. However it can be discussed on the basis of idealized trigonal bipyramidal (tbp) or square pyramidal (sp) geometrical models (having D_{3d} or C_{4v} symmetry respectively).[24] In this way these kinds of co-ordination compounds can be described as showing a given degree of tbp or sp character.[3,23]

The local copper environment in [Cu_2(terpy)$_2Cl_2$][PF_6]$_2$ is rather similar to that found in monomeric [Cu(terpy)-Cl_2]·H_2O.[3,10] In both compounds the co-ordination polyhedron around copper is well described as a deformed square-pyramidal conformation.[23–25] The longer copper-to-apical chlorine bond distance and the smaller copper out-of-plane displacement observed in the dimer can be understood in terms of repulsions between the monomeric [Cu(terpy)Cl]$^+$ entities that build up this complex cation. These monomeric entities lie roughly in parallel planes and are asymmetrically bridged by the chlorine atoms. The conformation corresponds, in terms of the classification proposed by Lintvedt *et al.*,[1] to 'type e' dimeric di-bridged complexes, with an ideal C_{2h} point group symmetry.

Various theoretical approaches have been developed in order to give an interpretation and to predict the magnetic behaviour of weakly interacting metal dimers.[26] All consider the empirical exchange parameter J in the HDvV hamiltonian to be constructed of two additive terms, corresponding to ferromagnetic and antiferromagnetic contributions respectively, that depend implicitly on the topology of the copper(II) ions in the dimers. The experimental sign of J is interpreted as the result of the competition of these two contributions.

In 'type e' complexes the spin density lies on parallel planes. The magnetic molecular orbitals are nearly orthogonal and their overlap is very small. Therefore intradimeric magnetic interactions are expected to be very weak.[27] On the other hand, for this topology type, all the terms in the equations obtained from the application of the perturbation theory[26] have a similar sensitivity to small variations of the dimer geometry. Thus these kinds of approaches lose their predictive or explanatory qualities about the ground state multiplicity (J sign).

The above considerations are supported by the structural and magnetic data concerning the di-μ-chloro bridged 'type e' copper(II) dimers already known and shown in Table 5. Notwithstanding that, Hatfield and co-workers[28,29] have pointed out that a smooth correlation exists relating the exchange parameter J and the Φ/R ratio (R being the longer

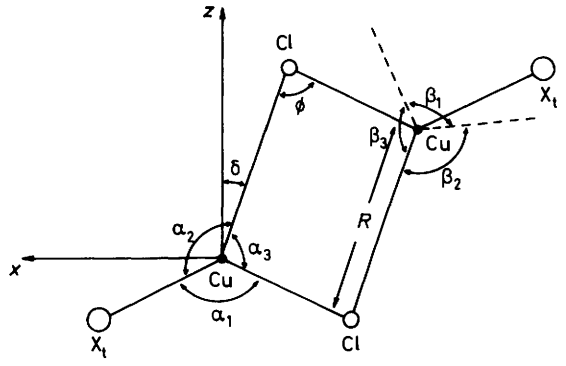

Figure 4. Representation of the various angles considered in Table 5

arguments account for the major frequency of the 'type e' dimers showing antiferromagnetic coupling.

Two significant departures from the sp geometry can be observed in all the complexes listed in Table 5. First, the basal-to-basal ligand angle values are different from 180°, indicating a displacement of the metal atom from the basal plane. The second one is the asymmetry on the apical-to-basal ligand angles (*i.e.* $\alpha_2 \neq \alpha_3$). The effect arising from the first deformation is the destabilization of the d_{xz} and d_{yz} metal orbitals both mixing in an antibonding way with the basal ligand orbitals and the concomitant stabilization of $d_{x^2-y^2}$ orbitals.[24a] The new ground state results from a mixture of these three orbitals, leading in this way to a spin density in d_{xy} orbitals that point to each other from each metal centre. The resulting direct exchange mechanism leads to an antiferromagnetic contribution that may stabilize the singlet state of the dimer. Moreover, the

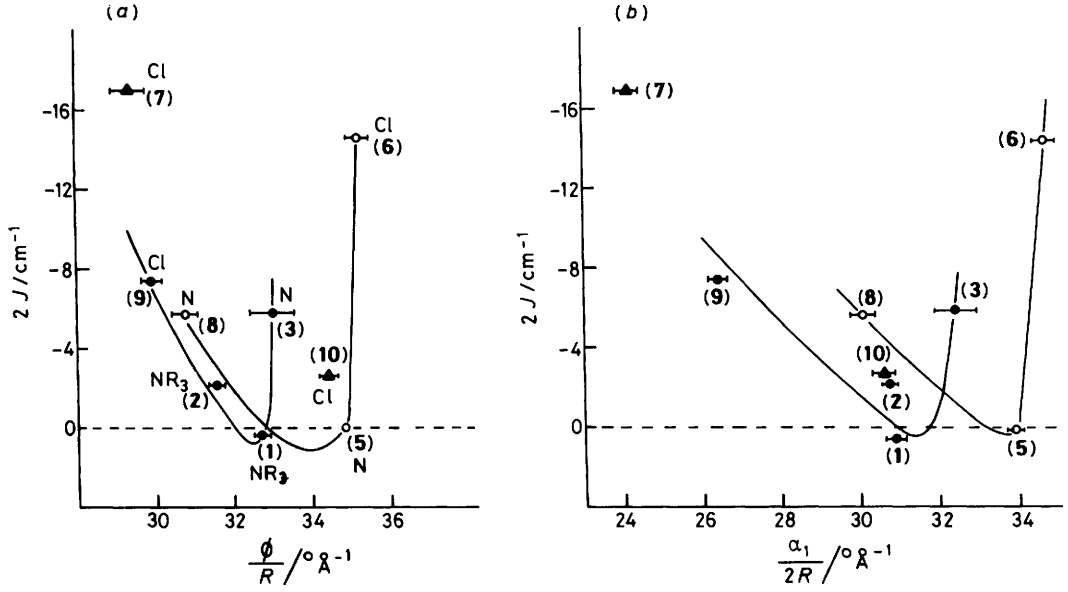

Figure 5. Variation of the J parameter (*a*) *vs.* Φ/R and (*b*) *vs.* $\alpha_1/2R$ (see Table 5 for the notations); ● = sp, ○ = spth, and ▲ = sptr geometry

Cu–Cl distance, that corresponds to the out-of-plane Cu–Cu bond in 'type e' dimers, and Φ the bridging angle; see Figure 4). This empirical correlation works well enough when a variety of dimeric topologies and bridging geometries are considered, and leads to a family of J *vs.* Φ/R curves depending on the bridging ligand nature.

It could be considered that this correlation reflects the relevance of the geometrical aspects of the bridge plane in the magnetic behaviour. This depends in fact on the nature and orientation of the molecular orbitals involved in the superexchange, which are very sensitive to the geometry of the copper(II) co-ordination polyhedron. As long as all the considered dimers hold a symmetry centre, they satisfy the expression $2\Phi = \alpha_1 + 2\delta$ relating the bridge angle to the angles that characterize the deviations of the actual dimer geometries in the bridge plane from those for an ideal square-planar dimer (Figure 4). For the latter the only antiferromagnetic exchange pathway comes from the direct interaction between the semi-occupied copper $d_{x^2-y^2}$ orbitals. All the other pathways, involving doubly occupied d_{z^2} and d_{xz} orbitals, lead to ferromagnetic coupling and the expected ground state will be the triplet one. Nevertheless, any symmetry lowering from C_{2h} may introduce new exchange pathways stabilizing the dimer singlet state. Moreover, variations of α_1 and δ from their ideal values (180 and 0° respectively), even though conserving the C_{2h} symmetry, induce the stabilization of the singlet state. All these d_{xz}–d_{xz} overlap may be enhanced by the asymmetry of the apical-to-basal ligand bond angles.

On the other hand, the co-ordination polyhedron around the copper atom in these types of compounds has been described as 'distorted square pyramidal' or 'distorted trigonal bipyramidal'. However, both from bond distances and angles, we consider that they are better described as 'regular square pyramidal' (sp) and 'tetrahedral or trigonal distorted square pyramidal' (spth and sptr, respectively) as Hathaway[25] has pointed out, characterized by the sets of bond angles listed in footnotes *b* and *f* of Table 5. Based on this and from the inspection of the structural data of Table 5 it is easy to classify the geometry of the copper environment in each compound. In this way compounds (**1**), (**2**), (**3**), and (**9**) show sp geometry, (**5**), (**6**), and (**8**) spth geometry, and (**7**) and (**10**) sptr. The copper–guanidinium dimer (**4**) is the only compound that shows tbp geometry.

Plotting J *vs.* Φ/R for the compounds belonging to each topological family, sp and spth (the number of sptr dimers is inadequate), gives a much better correlation than that found when they are all considered as included in the same structural class. This latter plot[28b] may well represent the envelope of the curves in Figure 5(*a*).*

Nearly similar trends are found in the plot of J *vs.* $\alpha_1/2R$

* The strong antiferromagnetic coupling of compound [{Cu(Hgua)-Cl_2}$_2$] (**4**) is as expected when the copper topology is tbp.[26d]

[Figure 5(*b*)]. This result represents the influence in these correlations of the effect from d_{xz} mixing in the ground state of copper(II) ions, that is directly related to the α_1 value (or the out-of-plane displacement) of the metals. The correlation based on the Φ values works probably because of the Φ–α_1 relationship stated above. The dimer magnetic properties depend mostly on the ground state of interacting ions and this in turn on their topologies. All the above arguments agree with this statement.

Another interesting point to be considered is the influence of the nature of ligands *trans* to the bridging one (see Figures 4 and 5). Of all dimers studied, those having a chlorine atom in a *trans* position show generally the greater antiferromagnetic interactions, and the lower J values are found in dimers having a *trans* aliphatic amine type of ligand. This observation agrees with the expected trend proposed by Hoffmann and co-workers[26c] about the influence of the electronegativity of substituents on superexchange interactions.

The electronic structure of the *trans* ligand and its donor–acceptor ability can modify the singlet–triplet energy gap. Thus, basic σ-donor ligands (as are the aliphatic amines) destabilize the antibonding $d_{x^2-y^2}$ magnetic orbital, with a concomitant decreasing of J due to a poor energy matching with the orbitals of the bridging atom. This argument accounts for the smaller J values of the dimers having a NR_3 *trans* ligand when compared with similar (same topology) *trans*-chlorine dimers. On the other hand, π-acceptor *trans* ligands (as are aromatic amines), remove electron density from the d_{xz} orbital, and the simultaneous destabilization of the antibonding $d_{x^2-y^2}$ and d_{xz} orbitals favours its mixing.

These arguments let us explain the greater antiferromagnetic character of the title compound with respect to most similar dimers having aliphatic amines as *trans* ligands.

As further magnetic and structural data concerning new compounds of this kind become available it will be possible to confirm the ideas put forward in this work.

Acknowledgements

This work was supported in part by a grant from the Comision Asesora de Investigacion Cientifica y Tecnologica, which we gratefully acknowledge.

References

1 R. L. Lintvedt, J. D. Click, B. K. Tomlonovic, D. P. Gavel, and J. M. Kuszaj, *Inorg. Chem.*, 1976, **15**, 1633.
2 D. J. Hodgson, *Prog. Inorg. Chem.*, 1975, **19**, 173.
3 T. Rojo, M. Vlasse, and D. Beltrán-Porter, *Acta Crystallogr., Sect. C*, 1983, **39**, 194.
4 (*a*) T. Rojo, J. Darriet, J. M. Dance, and D. Daniel-Porter, *Inorg. Chim. Acta*, 1982, **64**, 105; (*b*) J. M. Stewart, F. A. Kundell, and J. C. Baldwin, *X*-RAY 70 System, Computer Science Center, University of Maryland, U.S.A., 1970.
5 O. P. Anderson, B. J. Hathaway, D. E. Billing, and P. Nichols, *J. Chem. Soc. A*, 1979, 65.
6 T. Rojo, Ph.D. Thesis, University of Basque Country, 1981.
7 R. Allmann, W. Henke, and D. Reinen, *Inorg. Chem.*, 1978, **17**, 378.
8 M. I. Arriortua, T. Rojo, J. M. Amigó, G. Germain, and J. P. Declercq, *Acta Crystallogr., Sect. B*, 1982, **38**, 1323.
9 J. M. Savariault, T. Rojo, M. I. Arriortua, and J. Galy, *C. R. Acad. Sci. Paris, Ser. II*, 1983, **297**, 895.
10 W. Henke, S. Kremer, and D. Reinen, *Inorg. Chem.*, 1983, **22**, 2858.
11 S. Kremer, W. Henke, and D. Reinen, *Inorg. Chem.*, 1982, **21**, 3013.
12 E. Goldschmied and N. C. Stephenson, *Acta Crystallogr., Sect. B*, 1970, **26**, 1867.
13 F. W. D. Einstein and B. R. Penfold, *Acta Crystallogr.*, 1966, **20**, 924.
14 M. I. Arriortua, T. Rojo, J. M. Amigó, G. Germain, and J. P. Declercq, *Bull. Soc. Chim. Belg.*, 1982, **91**, 337.
15 T. Rojo, J. L. Mesa, M. I. Arriortua, and D. Beltrán-Porter, *An. Quím.*, 1984, **80**, 477.
16 V. Chomakern and K. N. Trueblood, *Acta Crystallogr., Sect. B*, 1968, **24**, 63.
17 J. H. Van Vleck, *Phys. Rev.*, 1948, **711**, 168.
18 D. W. McCall and D. C. Douglas, *J. Chem. Phys.*, 1960, **33**, 777.
19 G. Miller and H. S. Gutowsky, *J. Chem. Phys.*, 1963, **39**, 1983.
20 C. K. Harris, T. N. Lockyer, and N. C. Stephenson, *Aust. J. Chem.*, 1966, **19**, 1741.
21 J. S. Judge, W. N. Reiff, G. M. Intille, P. Baliway, and W. A. Baker, jun., *J. Inorg. Nucl. Chem.*, 1967, **29**, 1711.
22 C. M. Harris, T. N. Lockyer, R. L. Martin, H. R. M. Patil, E. Sinn, and I. M. Stewart, *Aust. J. Chem.*, 1969, **22**, 2105.
23 M. Vlasse, T. Rojo, and D. Beltrán-Porter, *Acta Crystallogr., Sect. C*, 1983, **39**, 560.
24 (*a*) A. R. Rossi and K. Hoffmann, *Inorg. Chem.*, 1975, **14**, 365; (*b*) E. L. Muetterties and J. L. Guggenberger, *J. Am. Chem. Soc.*, 1974, **96**, 1748.
25 B. J. Hathaway, *Coord. Chem. Rev.*, 1982, **41**, 423.
26 (*a*) G. Van Calkren, N. N. Smidt, and R. Block, *Phys. Status Solidi B*, 1979, **97**, 315; (*b*) O. Kahn and B. Briat, *J. Chem. Soc., Faraday Trans. 2*, 1976, 286; (*c*) P. J. Hay, J. C. Thibeault, and R. Hoffmann, *J. Am. Chem. Soc.*, 1975, **97**, 4884; (*d*) A. Bencini and D. Gatteschi, *Inorg. Chim. Acta*, 1978, **31**, 11.
27 W. E. Hatfield, *Comments Inorg. Chem.*, 1981, **1**, 105.
28 (*a*) E. Sinn, *Inorg. Chem.*, 1976, **15**, 2698; (*b*) W. E. Marsh, K. C. Patel, W. E. Hatfield, and D. J. Hodgson, *ibid.*, 1983, **22**, 511.
29 W. E. Marsh, W. E. Hatfield, and D. J. Hodgson, *Inorg. Chem.*, 1982, **21**, 2679.

Received 16*th December* 1985; *Paper* 5/2208